Analytica Chimica Acta 1037 (2018) 338–350

Contents lists available at ScienceDirect

Analytica Chimica Acta

journal homepage: www.elsevier.com/locate/aca

The influence of culture media upon observed cell secretome metabolite profiles: The balance between cell viability and data interpretability

Evangelia Daskalaki [a], Nicolas J. Pillon [b], Anna Krook [b], Craig E. Wheelock [a, *], Antonio Checa [a, **]

[a] Division of Physiological Chemistry 2, Department of Medical Biochemistry and Biophysics, Karolinska Institutet, Scheeles Väg 2, SE-171 77 Stockholm, Sweden
[b] Department of Physiology and Pharmacology, Integrative Physiology, Karolinska Institutet, von Eulers Väg 4a, SE-171 77 Stockholm, Sweden

HIGHLIGHTS

- The effects of five different media combinations were tested on the metabolic profiles of HEK293 and L6 cell lines.
- The media composition drives the cluster of the observed metabolic profiles on a media-specific basis.
- The addition of fetal bovine serum affects the observed metabolic profiles.
- Incubation affects the observed metabolic profile of cell-free media.
- Experimental design guidelines are proposed for cell culture secretome metabolomics studies.

GRAPHICAL ABSTRACT

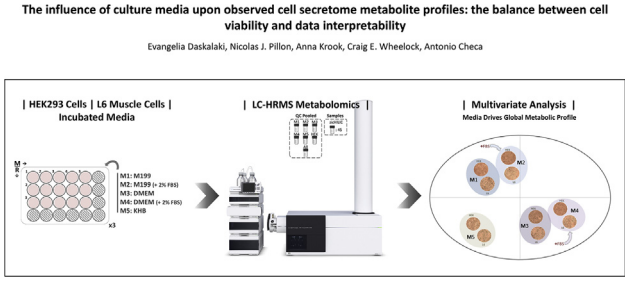

ARTICLE INFO

Article history:
Received 15 March 2018
Accepted 13 April 2018
Available online 18 April 2018

Keywords:
Secretome
Metabolomics
LC-HRMS
Cell media
FBS
Incubation

ABSTRACT

The application of metabolomics to investigating the cell secretome has garnered popularity owing to the method's large-scale data output, biochemical insight, and prospects for novel target compound discovery. However, there are no standardized protocols for the use of cell growth media, a factor that can exert profound effects upon the detected metabolites, and thus in the interpretability of the resulting data. Herein, we applied a liquid chromatography-high resolution mass spectrometry-based metabolomics approach to examine the influence of 5 different media combinations upon the obtained secretome of two phenotypically different cell lines: human embryonic kidney cells (HEK293) and L6 rat muscle cells. These media combinations were, M1: Medium 199, M2: Medium 199 + 2% fetal bovine serum (FBS), M3: Dulbecco's Modified Eagle's Medium (DMEM), M4: DMEM + 2% FBS and M5: Krebs-Henseleit Modified Buffer (KHB). The effect of incubation (37 °C) *vs.* refrigeration (4 °C) on DMEM medium over a 24 h period was also investigated. Results were validated for a selected panel of 5 metabolites measured from an additional cell culture experiment. Metabolomics identified a total of 53 polar metabolites that exhibited differential patterns on a cell type- and medium-specific basis. We observed that choice of media was the primary contributor to the secreted metabolite profile detected. The

* Corresponding Author.
** Corresponding author.
E-mail addresses: craig.wheelock@ki.se (C.E. Wheelock), antonio.checa@ki.se (A. Checa).

https://doi.org/10.1016/j.aca.2018.04.034
0003-2670/

addition of FBS resulted in unique detected metabolites, compared to media-only controls (M199 and DMEM alone). Glutamine and pyroglutamate were more abundant in incubated relative to refrigerated DMEM medium. The overall metabolic pattern of the metabolites from the targeted approach matched with that exhibited across M1-M5 of the metabolomics experiment, and aided in further identifying the presence of compounds that were below the limit of detection in metabolomics. Based upon these findings, we highlight the following considerations in designing a cell secretome-based metabolite profiling experiment: (1) multiple media combinations (with and without FBS) should be tested for each cell line to be investigated; (2) cell-free media combinations should be plated separately, and incubated/treated in the same experimental conditions as the cells; and (3) a compromise between cell death and metabolite detection should be identified in order to avoid batch-specific contributions from FBS supplementation.

1. Introduction

The cell is in many ways an intricate biochemical machine, with organizational structures that influence its collective driving force as a unit of life [1,2]. Ascertaining a blueprint of its phenotype begins with investigating the relatively small (<1200 Da) [3] labile metabolites, which act as fuel in this complex machine. The number of metabolites within a given system are dependent upon the number of unique cell-specific metabolomes interacting together [3–5]. Metabolomics provides a platform to analyze large-scale phenotypic changes in the cell, with liquid chromatography coupled to mass spectrometry (LC-MS) being the commonly employed technique. LC-MS enables metabolite detection from both intra- (*i.e.,* cell lysates), and extra-cellular (*i.e.,* cell secretome) matrices. From a practical stand-point, the use of cell cultures in both health and disease models provides a relatively cost-efficient approach, benefiting from controlled experimental environments, as well as less arduous ethical procedures in comparison to animal/human experiments. However, 2-D cell models can result in bioactivities that deviate from the *in vivo* response, which has resulted in the development of 3-D or spheroid cell models [6]. From a scientific perspective, the creation of novel network models (*i.e.*, from the metabolomics data), may also help to elucidate a drug's mode of action, cell to cell signaling, as well as provide new markers associated with cell toxicity [7,8].

In spite of the unique prospects of combing cell culture analysis with metabolomics, the physicochemical properties of the intra and extracellular matrices (the latter includes the media) provide formidable analytical challenges [9,10]. Detailed sample preparation methods available within industry in relation to cell culture biotechnology have already been described in detail by Causon and Hann [9]. Beyond the quenching and harvesting of cells, one major component remains when investigating the cell secretome - this being the growth media. To maintain cell growth and viability, cells are propagated in specific growth media. Culture media provides cells with sources of energy and specific compounds that regulate the cell cycle, often including amino acids, vitamins, inorganic salts, and glucose. Media content also serves to maintain pH and osmolality. In addition to growth media, most mammalian cells also require serum supplementation - with fetal bovine serum (FBS) being the most common [11]. Serum provides cells with growth factors, hormones, and attachment factors, but has the disadvantage of having an undetermined composition, which varies from batch to batch. Compounds present in either serum or culture media may potentially mask the secreted metabolites released from the cells, ultimately obscuring the profile of the secretome. An example of this analytical challenge has been noted by Creek et al. [10], whereby common supplemented media (HM11) utilized to investigate drug-induced changes in the parasite metabolome of *T. brucei* are often too enriched and therefore do not adequately reflect the *in vivo* environment of the bloodstream form of *T. brucei*. The authors proposed an adapted growth medium to ensure viability of the cells grown *in vitro*, without obscuring the desired metabolite pattern, which was guided by a non-targeted metabolomics approach (LC-MS) of the cell extracts. This could potentially be translated to the cell secretome; however, this has yet to be investigated. Another question remains regarding the use of serum. Nonnis et al. [11] utilized a LC-MS/MS approach to observe the variations in growth media combined with different concentrations of FBS (0%, 5%, and 10%) on the number of proteins in the cellular secretome of mesenchymal stromal cells (human bone marrow). The authors suggest supplementing with FBS until desired confluence, and then transferring to a serum-free medium-only environment for cell secretome collection in order to reduce analytical interferences.

Another example of an analytical challenge is in the variability exhibited across conditioned media, which is a medium containing all molecules released by cells. MacIntyre et al. [12] utilized a ^{1}H Nuclear Magnetic Resonance (^{1}H NMR)-based metabolomics approach to profile conditioned media from human foreskin fibroblasts that are used as a supplement in *in vitro* cell culture studies of human embryonic stem cells. The authors showed the effect of conditioned media on the secretory *vs.* utilization of metabolites at differing cell passaging stages [12]. Interestingly, conditioned media also evidenced metabolic changes after 2 weeks of storage at −20 °C [12].

In an attempt to apply metabolomics to the cell secretome, it becomes evident from the literature that there is no standardized method when it comes to the use of media, which is also highly dependent on which cell lines are investigated [13,14]. In the present work, we aimed to determine this variability, as well as the complex experimental outcomes induced by growth media in the cell secretome. We used LC-high resolution mass spectrometry (HRMS) based metabolomics to inspect the influence of 5 different media combinations in the obtained secretome of two phenotypically different cell lines (human embryonic kidney cells and L6 rat muscle cells). We also investigated the effect of incubating (37 °C) *vs.* refrigerating (4 °C) the same medium over a 24-h period. Finally, results were validated using a targeted panel of metabolites. We observed a strong influence from the different media combinations on the resulting cell metabolic profile and based upon these findings we propose considerations for designing cell culture media metabolomics studies.

2. Materials and methods

2.1. Cell culture and sample preparation

2.1.1. Cell culture and test media

Rat L6 muscle cells (ATCC, CRL-1458) were grown in α-MEM (12,571–063, Lot: 1865286). Human embryonic kidney cells (HEK293, ATCC, CRL-3022) were grown in Dulbecco's Modified Eagle's Medium (DMEM + GlutaMAX™). Media were supplemented with 10% FBS (F7524, lot 084M3250; Sigma Aldrich) and 1% Antibiotic Antimycotic Solution (Sigma Aldrich 15,240–062, lot: 1851596). For seeding, cells were washed with phosphate buffered saline (PBS) and suspended by incubation with trypsin for 5 min. Cell suspensions were counted and cells diluted to 100,000 cells mL^{-1}. In a 24-well plate, 500 μL of each cell suspension was added per well. After seeding, L6 cells were allowed to grow until confluence and differentiated into myotubes by switching to α-MEM supplemented with 2% FBS to induce fusion. Myotubes were used for the experiment 5 days after the initiation of differentiation. HEK293 cells were seeded two days before the experimental day. Antibiotics were removed 24 h before the experiment. Cells were then washed once with PBS before adding 300 μL of test media for 24 h. The test media included were as follows, M1: Medium 199 (31,150–022, Lot: 1838981; Invitrogen), M2: Medium 199 plus 2% of FBS, M3: DMEM (21,885–025, Lot: 1858632; Invitrogen), M4: DMEM + 2% FBS, and finally M5: Krebs-Henseleit Modified Buffer (KHB) that was made in-house from powders. Formulation of the media can be found in Table S1. Numbers of test media (M1-5) correspond to their position on a 24-well plate as are indicated in the workflow schematic of Fig. 1. In total, three 24-well plates were utilized for this experiment. Each cell type was incubated at 37 °C in a separate plate with the five different test media in triplicate, positions of which are shown in Fig. 1. The third plate had the 5 different media combinations without the cells, incubated in the same experimental conditions as the cells, and were inserted in the same well positions as outlined in Fig. 1. This provided a total number of 45 samples (*i.e.,* 15 samples per plate).

2.1.2. Sample extraction and quality control preparation

Immediately after the incubation period, 200 μL of each sample was transferred into a clean Eppendorf tube and centrifuged for 2 min at 19,000 *g* in order to remove any debris. Then, 100 μL was subsequently transferred to a new Eppendorf tube. Next, 350 μL of ice-cold methanol was added and samples were vortexed for 30 s. Samples were then incubated at room temperature for 10 min before centrifuging for 15 min at 12,000 *g*. Finally, 150 μL from the supernatant was transferred into an LC vial for analysis. Another 150 μL was stored at −80 °C as backup. Additionally, 150 μL of refrigerated medium was also removed and processed as described above for analysis. One LC vial was prepared for each medium type and injected in triplicate.

Three types of quality controls (QC) were prepared by pooling 25 μL of the samples representing: 1) samples from each medium separately (QC-M1-5), 2) the 15 samples from the HEK293 incubated plate (QC-HEK), and 3) one for all 45 samples (QC-All). After vortexing, 150 μL were transferred into LC vials for analysis. The workflow schematic of the sample preparation procedure is summarized in Fig. 1.

2.1.3. Cell viability and cell death assays

To measure cell death, 40 μL from the cell supernatant was transferred to a clean plate, and lactate dehydrogenase (LDH) activity was measured in duplicate by following the manufacturer's instructions (In Vitro Toxicology Assay Kit, Lactic Dehydrogenase based, Sigma-Aldrich TOX7). For the validation study, at the end of the incubation, 3 μL of 10% Triton X100 was added in a few wells as a positive control for maximal cell lysis. Viability was determined via a Thiazolyl Blue Tetrazolium Bromide (MTT) assay. Briefly, 300 μL of MTT (Sigma Aldrich M2128, 0.5 mg mL^{-1} in DMEM) was added per well and cells incubated at 37 °C for 1 h. MTT crystals formed in the cells were dissolved by adding 500 μL dimethylsulfoxide and mixing on a shaker for 2 h. Lysates were transferred into a clean 96-well plate and absorbance read at 550 nm in a microplate reader. See Fig. 1 for the cell viability workflow schematic. Cell morphology, before and after the addition of M1-5, was evaluated through images taken on a Leitz inverted microscope with x 50 magnification.

2.1.4. Incubated vs. non-incubated DMEM + GlutaMAX™

DMEM medium without FBS (M3; same bottle as original experiment) was placed in each well of two plates (N: 15 × 2) in the same position as the experimental samples depicted in Fig. 1. One plate was incubated at 37 °C, and another refrigerated at 4 °C for 24 h. All preparation was conducted in sterile conditions, exactly as for the original cell culture experiment. The weight of each plate was measured prior to and immediately after the 24-h period, after which time the same preparation technique, instrumentation as well as processing method was used as previously outlined. Quality controls were prepared to represent all samples (QC-All). Incubated and non-incubated samples were injected in randomized order to facilitate direct comparison. The QC-All were injected at the beginning and end of the run as well as after each batch of 10 samples.

2.2. Mass spectrometry data acquisition

2.2.1. Reagents and chemicals

LC-MS grade water and formic acid (Optima®-LC/MS) were purchased from Sigma-Aldrich (St. Louis, USA). Acetonitrile (Optima®-LC/MS), and methanol (Optima®-LC/MS) were purchased from Fisher-Scientific (Loughborough, UK). For the LC-HRMS experiments, the internal lock masses (purine and HP-0921) and tune mix for calibrating the Q-TOF-MS (ESI-low concentration tuning mix) were purchased from Agilent Technologies (Santa Clara, USA). Arginine, citrulline, ornithine, folic acid, methionine, N_4-arginine, C_5-folic acid and d_3-methionine standards were purchased from Sigma-Aldrich.

2.2.2. LC-HRMS metabolomics

LC-HRMS experiments were performed on a 1290 Infinity II ultra-high performance liquid chromatography (UHPLC) system coupled to a 6550 iFunnel quadrupole-time of flight (Q-TOF) mass spectrometer equipped with a dual AJS electrospray ionization source (Agilent Technologies, Santa Clara, CA, USA). Polar metabolites were separated on a SeQuant® ZIC®–HILIC (Merck, Darmstadt, Germany) column 100 Å (100 mm × 2.1 mm, 3.5 μm particle size) coupled to a guard column (20 mm × 2.1 mm, 3.5 μm particle size) and an inline-filter. Mobile phases consisted of 0.1% formic acid in water with (solvent A) and 0.1% formic acid in acetonitrile with (solvent B). The elution gradient used was as follows: isocratic step at 95% B for 1.5 min, 95% B to 40% B in 12 min and maintained at 40% B for 2 min, then decreasing to 25% B at 14.2 min and maintained for 2.8 min, then returned to initial conditions over 1 min, and the column was equilibrated at initial conditions for 7 min. The flow rate was 0.3 mL min^{-1}, injection volume was 2 μL and the column oven was maintained at 25 °C.

Two independent injections were run for positive and negative acquisition modes. The Q-TOF MS system was calibrated and tuned according to the protocols recommended by the manufacturer. Nitrogen (purity > 99.9990%) was used as a sheath gas and drying

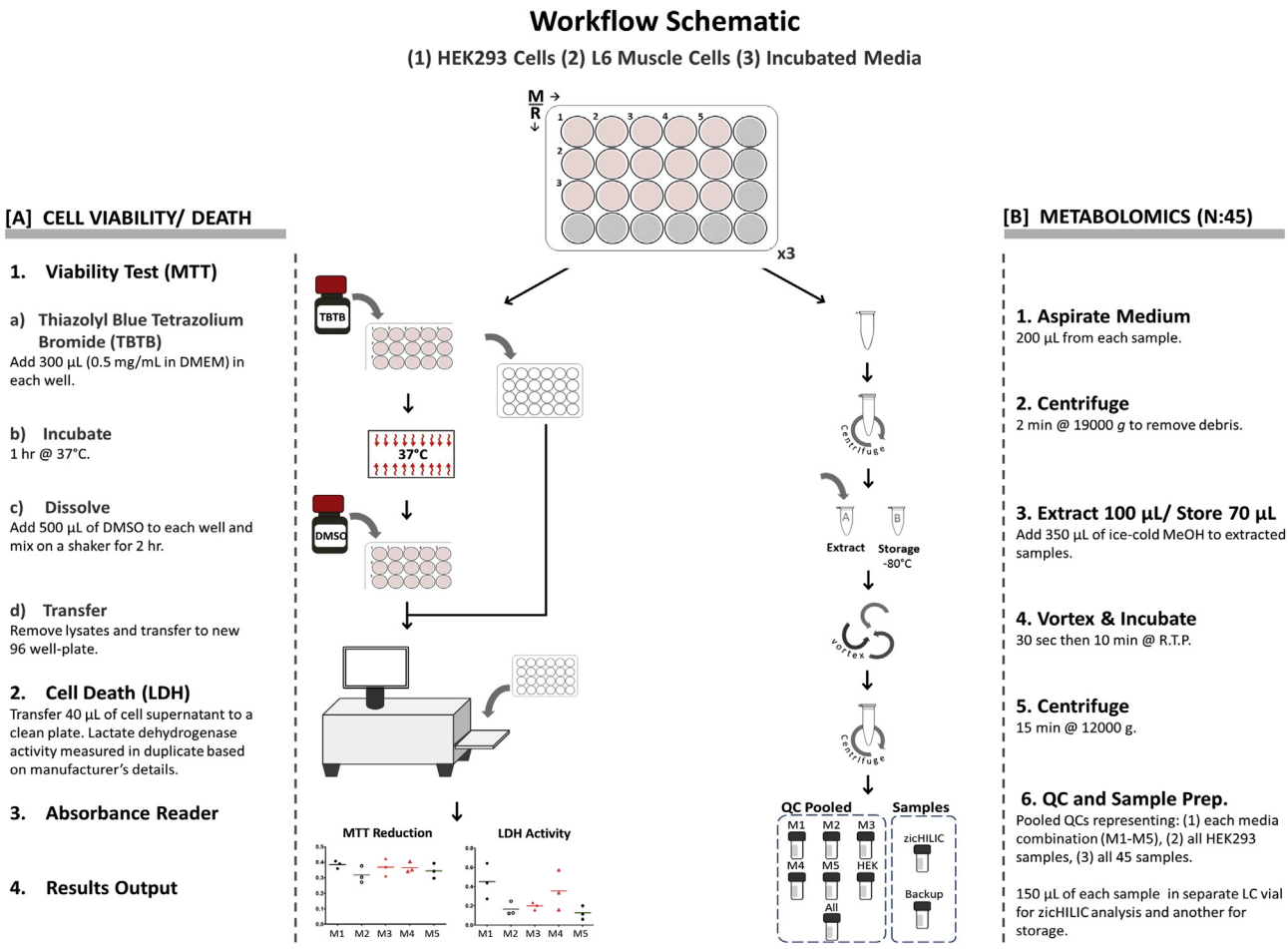

Fig. 1. Workflow schematic of cell viability/death assays (A), and metabolomics (B) sample preparation stages. Three 24-well plates were prepared separately for the HEK293 and L6 cell lines, as well as for the five different media combinations (M1-5) without cells. M1-5 represent the position of the five different media combinations, and R denotes the number of replicates per sample type. There were three replicates per medium type, providing a total number of 45 samples. MTT: Thiazolyl Blue Tetrazolium Bromide; LDH: lactate dehydrogenase; DMEM: Dulbecco's Modified Eagle's Medium; DMSO: dimethylsulfoxide; MeOH: methanol; R.T.P.: room temperature and pressure; QC: quality control.

gas at a flow of 8 L min^{-1} and 15 L min^{-1}, respectively. The drying and sheath gas temperature were set at 250 °C, with the nebulizer pressure at 35 psi and voltage 3000 V (+/− for positive and negative ionization mode, respectively). The fragmentor voltage was set at 380 V. The acquisition was obtained with a mass range of 50–1200 *m/z*, where full scan high-resolution data were acquired at three alternating collision energies (0 eV, 10 eV and 30 eV). The data acquisition rate was 6 scans sec^{-1}. Between 16 and 25 min, LC flow was diverted to the waste. For further details regarding the acquisition methodology please see Naz et al. [15].

The primary analytical sequence was prepared to ensure randomization of samples based on medium type. Each QC was injected in triplicate. All HEK293 samples were re-injected at the end of the sequence, in randomized order, in order to compare with those injected throughout the sequence, but separated by medium type. The QC-All samples were run at the beginning, and at the end of the primary sequence, as well as a third time at the end of the final HEK293 set. One aliquot of each media (M1-5), that was not incubated, was prepared as previously described and injected in triplicate throughout the sequence based on media type. Methanol (MeOH) blank samples were injected at the beginning, and end of the sequence. Please see Fig. S1 for a visual representation of the sequence planning.

Positive and negative raw LC-HRMS files were independently processed with an in-house developed PCDL library for polar metabolites (n = 225) using Profinder version B.06 (Agilent Technologies) [15]. Proper identification of reported compounds (n = 53) was assessed by accurate mass and retention time (AMRT) plus fragment identification at two collision energies (10 and 30 eV) using an in-house generated database as previously described [15]. For the M3 media incubation experiment, a new PCDL library including only the metabolites previously identified in this medium was used.

2.2.3. LC-MS/MS targeted analysis

Targeted LC-MS/MS analyses were performed on an ACQUITY UPLC System from Waters Corporation (Milford, MA, USA) coupled to a Waters Xevo® TQ-S triple quadrupole system equipped with an Electrospray Ion Source. Separation was carried out on a SeQuant® ZIC®–HILIC (100 × 2.1 mm, 3.5 µm, 100 Å) column equipped with a SeQuant® ZIC®–HILIC guard column (20 × 2.1 mm), both from Merck. Mobile phases consisted of 0.1% formic acid in water (aqueous) and 0.1% formic acid in acetonitrile (organic). The elution gradient used was as follows: 0.0 min, 95% B; time range 0.0–2.0 min, 95% → 80% B (linear decrease); time range 2.0–7.5 min, 80% → 40% B (linear decrease); time range 7.5–11.5 min, 40% → 25% B (linear decrease); time range 11.5–13.0 min, 25% B (isocratic step); time range 13.0–13.2 min, 25% → 95% B (linear increase) and 13.2–17.0 min, 95% B (isocratic column conditioning). The flow rate was set at 300 µL min^{-1}, the

injection volume was 2.5 μL and the column oven was maintained at 27 °C. Detection was performed in positive ionization mode. A quantifier and qualifier SRM were acquired for all compounds as described in Table S2. Samples were injected following the same order as in the LC-HRMS experiment previously described, but without a repeated injection for HEK293 samples at the end of the sequence. For targeted analyses, the methanol crash solution contained a mix of internal standards ($^{15}N_4$-Arginine, $^{13}C_5$-Folic acid and d_3-Methionine). For relative quantification, the ratio between the areas of each compound and its appropriate internal standard (Table S2) was calculated. For additional confirmation, the ion ratios between the quantifier and qualifier ions (maximum deviation = 20%) were calculated.

2.3. Statistical analysis

Only metabolites detected in at least two of the replicates were included in further analysis. The missing value from the third replicate, for individual metabolites, was replaced by 25% of the minimum peak area of that metabolite across all samples. A missing value, in this instance, refers to falling below the limit of detection (LOD). In total, the number of replaced values did not exceed 1%. Metabolites detected in both ionization modes were correlated, and the ones with a larger relative intensity as well as lower %RSD value from the QC-All samples were selected. Principal component analysis (PCA) and partial least squares discriminant analysis (PLS-DA) were performed on univariate (UV) scaled data using SIMCA v 14.0 (MKS Umetrics, Sweden). Student's *t*-test, as well as bar chart generation, were conducted in Excel (Microsoft Office). Other graphical representations were generated via GraphPad Prism (GraphPad software, Inc.), and R v 3.4.0 (R Development Core Team, Vienna, Austria). For the targeted validation study, metabolite data are presented as response values, which refers to the ratio between the area of the identified compound and its corresponding internal standard. The response values were log transformed (base of 10) and scatter plots generated with Excel. Given that the response value is always below 1, the resulting values are negative. A one-way ANOVA with Dunnett's Multiple Comparison Test was performed on the LDH as well as the MTT assay data, with M4 (DMEM + FBS) used as the control (GraphPad software, Inc.).

3. Results and discussion

Cell culture studies employ a diverse range of experimental protocols that involve multiple variables including composition of the medium, quantity and composition of added serum, incubation time, incubation temperature, and eventual washing with for example PBS. This variability in experimental protocols is likely to affect the observed metabolic profiles secreted by the cells. In order to provide a rigorous description of these effects, we performed a series of experiments in which we adapted a standardized culturing protocol using two phenotypically diverse cell lines derived from humans and rats. The HEK293 cell line, derived originally from human kidney embryonic cells, is a widely used model within cell biology, biotechnology and bio-therapeutics [16]. The L6 rat (*Rattus norvegicus*) myotube cell line from skeletal muscle is a commonly used model to investigate, for example, insulin stimulation and glucose transport efficiency [17]. In order to rigorously compare the effects of culturing conditions upon observed metabolic profiles, the pre-analytical steps of sample preparation were kept to a minimum allowing us to quench metabolism post-incubation, as well as precipitate the protein content without compromising the sample itself. FBS is generally added to cell cultures in order to sustain growth; however, it alters the physicochemical and rheological properties of the cultured media [18]. There are additional components within the serum [19], such as growth factors, metabolites and proteins that contribute to the overall number of detected metabolites. Hence, FBS was chosen as an additive at 2% to the two main rich media types- M199 and DMEM. Based on the manufacturer details, the number of organic compounds in M199 and DMEM are 53 and 26, respectively. The KHB medium is a depleted medium of only 2 organic compounds, the remaining being inorganic salts (details of the three selected media are provided in Table S1).

3.1. Incubated vs. control non-incubated medium

PCA score plots were generated to observe the distribution of samples between the control non-incubated media (Fig. 2. A), as well as the 24-h incubated media (Fig. 2. B). The control non-incubated media, injected from the same LC vial, clustered according to medium type. However, the incubated media M1-4, showed variability across their respective replicates. This observation was not observed for M5, which can be justified by the low number of reported organic compounds in this medium.

3.2. General overview of detected metabolites

Based on our metabolomics approach, the total number of detected metabolites across all experimental conditions was 44 and 27 in positive and negative ionization modes, respectively. Correlation of the overlapping metabolites, and %RSD calculation of the QC-All samples, allowed for assignment into either positive or negative datasets. This resulted in 53 uniquely confirmed metabolites (43 in positive and 10 in negative, Table S3), with the most common metabolite class detected being the amino acids, peptides, derivatives and analogues (45%). Additional class assignment is shown in Fig. 3 (D).

Venn diagrams were created for each media combination separately (Fig. 3A–C), highlighting the unique and overlapping number of metabolites in each cell type, as well as control incubated medium. The total number of detected metabolites for each medium comparison, without FBS, resulted in 50, 47 and 43 metabolites for M1, M3 and M5, respectively. The addition of FBS raised the total overlapping number of detected compounds (M2: 38 and M4: 38) relative to the control incubated media. This was followed by a reduction in the cell specific number of detected compounds by > 50% (from 13 (M1) to 6 (M2), and from 16 (M3) to 6 (M4) (Fig. 3 A-B). In the depleted media (KHB, M5) 70% of the compounds (30 out of 43) were uniquely detected in the cell secretome of HEK293 and L6 cells (Fig. 3. C).

3.3. Cell viability and lysis

Fig. 4 Displays the effect of the different media before and after incubation with HEK293 (Fig. 4A) and L6 (Fig. 4B) cells along with their death and viability. LDH is an enzyme localized in the cytoplasm of the cells. Upon cytosolic membrane damage, LDH is released in the supernatant of the cells and can therefore be used to estimate cell death. Complementarily, MTT is metabolized by NAD(P)H-dependent oxidoreductases and therefore reflects the viability of the cells. In HEK293 cells, none of the media affected cell viability and only medium M1 and M4 had slightly elevated cell death, which was not significant. In L6 cells however, the composition of the medium had a stronger effect. The most striking effect was the significant increase in cell death (LDH) in M1, M3 and M5. This suggests that withdrawal of FBS was a significant stress for the L6 cells. Cell death triggers the release of cytoplasmic content into the conditioned medium and can therefore be an important confounding factor. However, LDH activity did not correlate with the

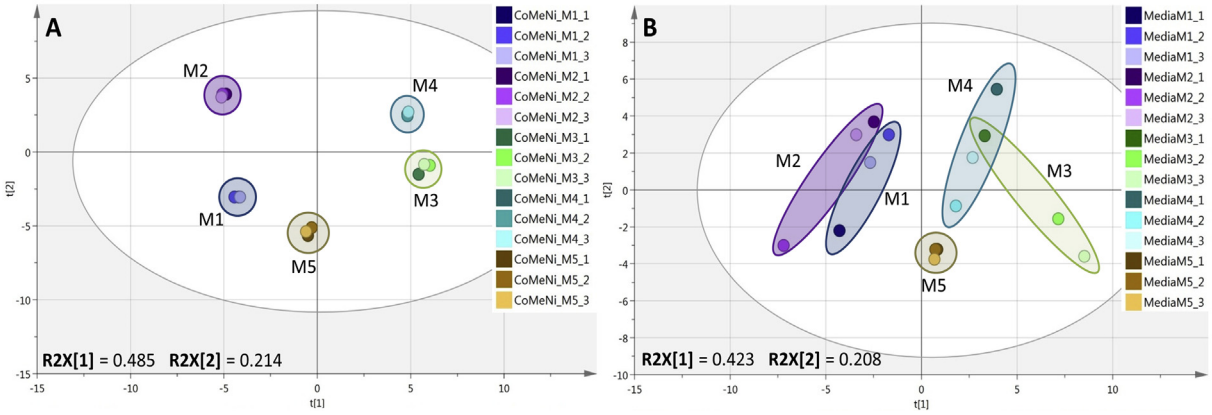

Fig. 2. Score plot comparison of control non-incubated and incubated media with combined data from positive and negative ionization modes. **A.** Score plot of control media (n = 3). All triplicates cluster depending upon medium type. **B.** Score plot of incubated media showing variability between the replicates representing each medium (n = 3). Circles around each cluster of samples are simply used for visual purposes and do not represent any statistical value (*e.g.*, 95% confidence interval).

number of detected metabolites, maybe due to the masking effects of metabolites contributed by FBS. We also observed that in M2 there were no cell-specific metabolites in contrast to the other media combinations (Fig. 3). In the L6 cells, M5 showed a significantly lower cell viability compared to M4 (control), and the highest significant cell death, as previously mentioned, was exhibited in M1, M3 as well as M5 - this cannot be discerned by the preliminary metabolite overview of the Venn diagrams. Overall, viability and cell death remained within an acceptable range, and the metabolic analysis was not significantly affected by the potential release of cytoplasmic content in the supernatant.

3.4. Differences in metabolites observed in HEK293 vs. L6 cells

PCA was performed to profile the secretome of our selected cell lines. HEK293 and L6 showed distinct medium-specific clustering as shown in the score plots (Fig. 5A and C), exhibiting the same directional pattern in both cases in terms of location of these media clusters. From this analysis we can discern that the medium itself drives the global profile observed in the score plots. Furthermore, both M1-M2 and M3-M4 clustered close together showing a minor influence of 2% FBS addition to the media.

Creatinine, creatine, taurine, malic acid, allantoin, citric acid and uridine were detected only in media supplemented with 2% FBS. None of these metabolites are present in the manufacturer's formulation of M199 or DMEM. It is therefore likely that these compounds originated from FBS itself. Given the complex nature of FBS, it is fair to assume that there will be some degree of contribution at the metabolite level and that this contribution will be specific to the batch of FBS used [20]. Hence, some cell death may be deemed a viable compromise, when combining with a metabolomics platform. In fact, in the ^{1}H NMR study by MacIntyre et al. [12], two compounds, 2-hydroxybutyric acid and 2-hydroxyisovaleric acid, were detected in the unconditioned media, yet they did not appear in the manufacturer's commercial formulation.

Due to the fact that different media and cell types can affect chromatographic and MS performance, HEK293 samples were injected twice throughout the sequence, once randomized by cell type and once randomized by media type (Fig. S1). The observed clustering of samples in the score plot shown in Fig. 5 (B) indicates that there were no instrumental interferences (*e.g.*, injection order or media type). As expected, given the depleted nature of M5, the samples incubated with this media clustered independently from M1-4 in the PCA scores plot. Finally, the distribution of medium-specific QCs, as well as the QC-All, in the PCA score plot showed similar patterns of clustering, confirming that there were no visible sequence related issues (Fig. 5. D).

3.5. Example metabolite pattern

Five metabolites from positive and three from negative ionization acquisition modes were selected as examples to highlight the metabolic variability across the two cell types (Fig. 6.). These eight compounds were selected in order to cover the different patterns observed across all the detected metabolites. The purpose of the current study was to investigate how differences in media composition (with or without FBS) translate to the detected secretome, rather than directly compare the two cell types together. Accordingly, the following data presentation focuses on the effects of media composition upon metabolite levels, not cell type-specific differences. To facilitate graphical visualization and comparisons, $\log_{10}$ of the peak areas are presented. Non-detected compounds are presented as 0 values. Although the precise limit of detection in a metabolomics experiment cannot be determined, we estimated its value for visualization reasons and present it as a shaded area in the metabolite panels. The original non-transformed data are provided in Supplementary Data.

Cytosine was only detected in L6 cells incubated media (between 5.5 and 6.1 $\log_{10}$ [Peak Area]). Therefore, this represents a metabolite that has been secreted into the extracellular matrix in a cell type-dependent manner. Conversely, guanine was only secreted by HEK293 cells (between 6.0 and 6.6 $\log_{10}$ [Peak Area]) and only observed in M199 medium (between 4.9 and 5.3 $\log_{10}$ [Peak Area]), suggesting an uptake of guanine by L6 when it was available. In order to ensure the presence of guanine in the secretome, this profile suggests that DMEM is the most suitable for this particular set of cells, along with the depleted medium (M5). In contrast to glucose, asparagine and fumarate were only detected in the cells (both L6 and HEK293). Proline evidenced a consistent level in both cell lines (between 7.0 and 7.5 $\log_{10}$ [Peak Area]), with deviations observed across the media combinations alone. Proline was not included in the medium formulation of DMEM, hence its detection may be a result of other unknown factors. In this example, differential secretion of proline into the media was better detected with M3-M4 or M5 media. Glucose, on the other hand, is an example of a metabolite highly abundant in all controls, as it is added to each growth medium. Thus, the decreased relative peak

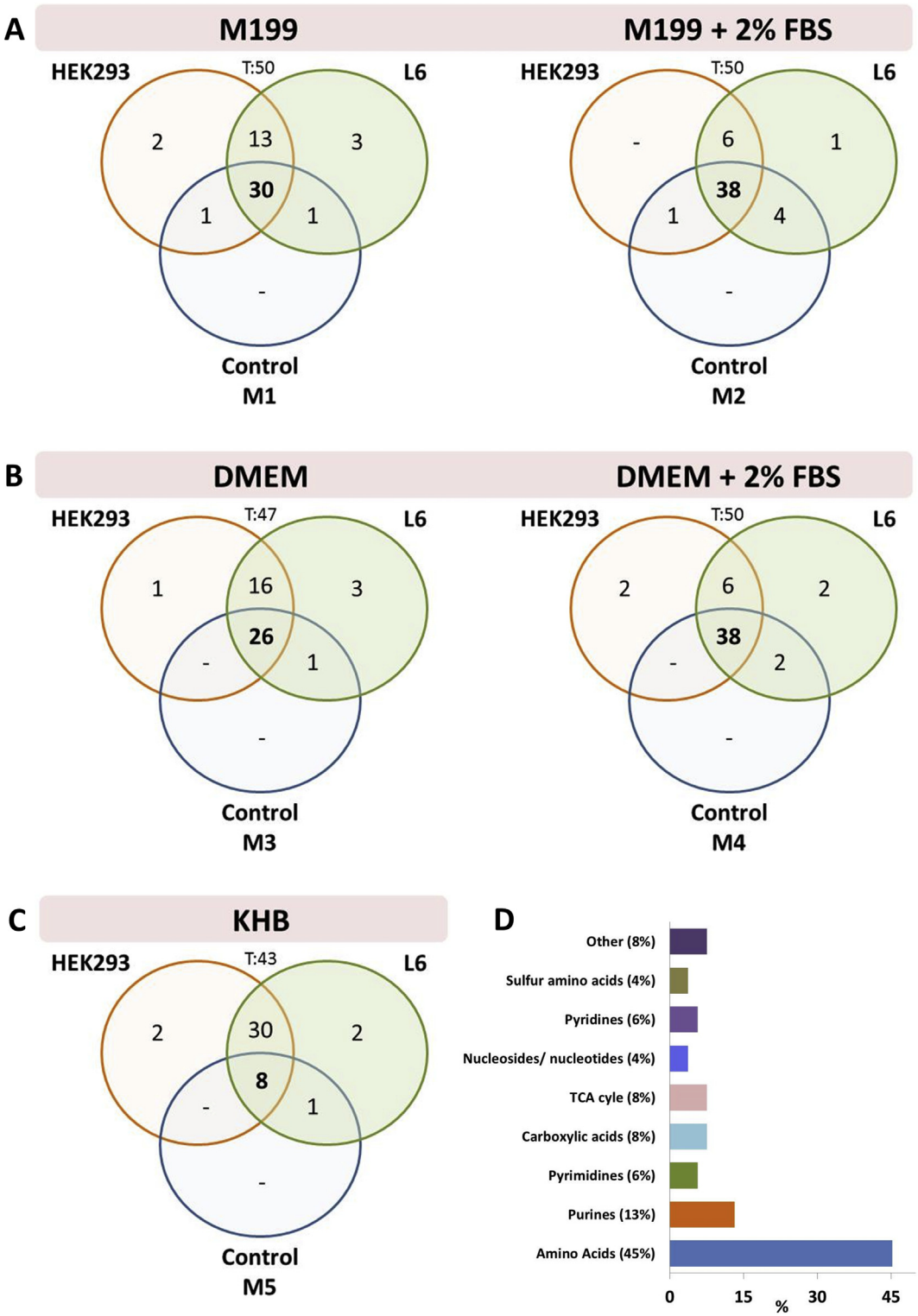

Fig. 3. Comparison of detected metabolites in HEK293 and L6 cells for each media combination (M1-5). **A.** Venn diagrams of HEK293 cells, L6 cells and control non-incubated media DMEM + GlutaMAX™ alone (M1) and with 2% fetal bovine serum (FBS) (M2). **B.** Venn diagrams of the cell secretomes and the control non-incubated media M199 alone (M3) and with 2% FBS (M4). **C.** Venn diagram of the cell secretomes along with the depleted KHB non-incubated media. **D.** Bar graph representing metabolite class overview of 53 detected compounds in positive and negative ionization acquisition modes. Class names have been shortened, complete names are: amino acids, peptides, derivatives and analogues (45%); purine, purine nucleosides, and derivatives (13%); pyrimidines, pyrimidine derivatives and pyrimidine nucleosides (6%); carboxylic acids and derivatives (8%); TCA cycle metabolites (8%); nucleosides, nucleotides, and analogues (4%); pyridines and derivatives (6%); sulfur amino acids (4%); and other (*i.e.*, hexose, hydroxypyrimidine, imidazopyrimidines, azole; 8%). T denotes the total number of detected metabolites for that comparison. DMEM: Dulbecco's Modified Eagle's Medium, M199: Medium 199, KHB: Krebs-Henseleit Buffer.

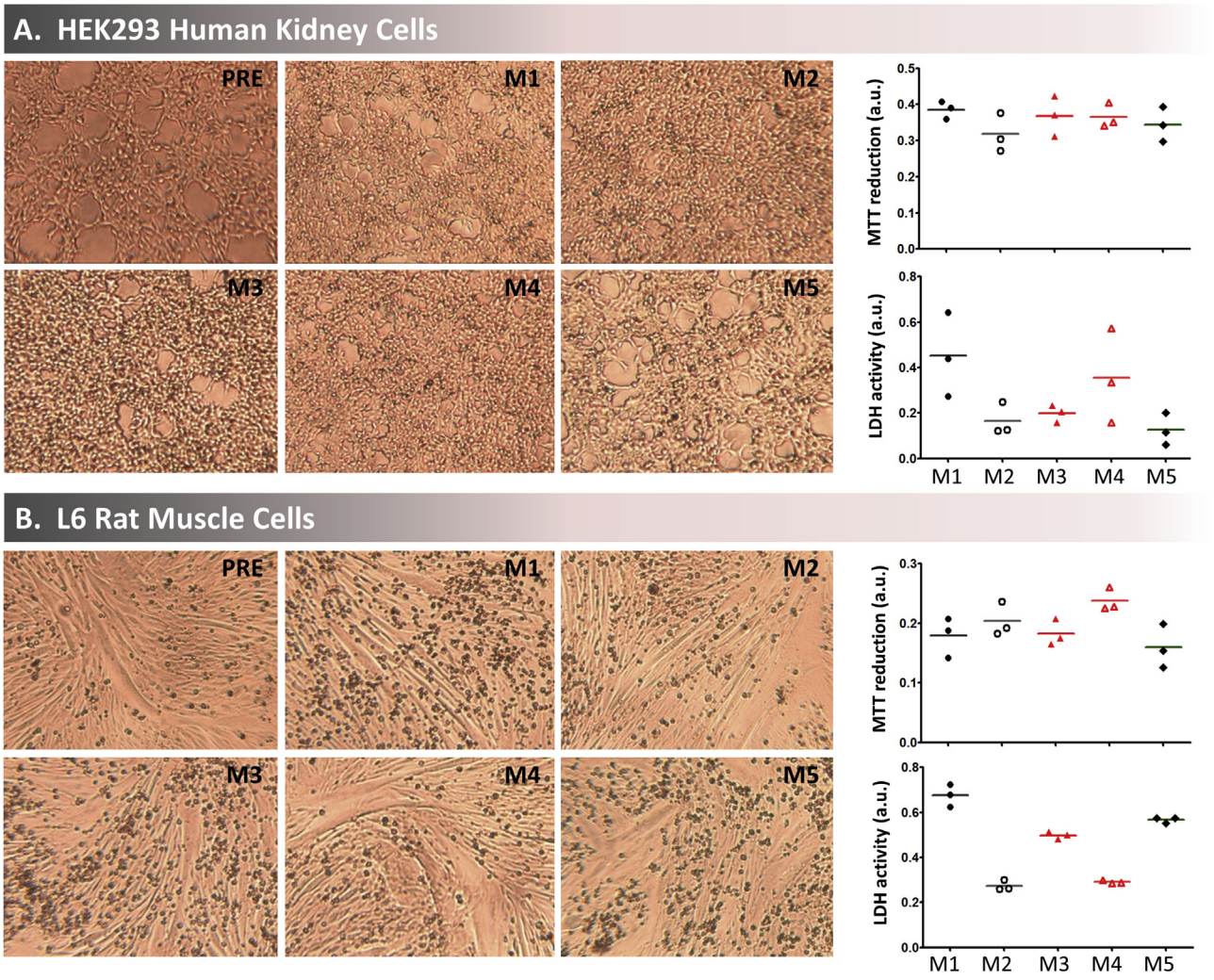

Fig. 4. Cell viability and death assays. **A.** HEK293 cell images before (PRE) and after incubation in the different media combinations. M1: M199, M2: M199 + 2% FBS, M3: DMEM, M4: DMEM +2% FBS, and M5: KHB. Increased MTT reduction signifies better cell viability, and an increase in LDH activity correlates to enhanced cell death. There were no significant changes in MTT or LDH activity. **B.** L6 cell images before and after incubation with the different media, followed by cell viability and death assays. Compared to the control (M4), M5 exhibited a significantly lower cell viability based on the MTT assay (adjusted *p*-value: 0.0247). M1 as well as M3 and M5 had significantly higher cell death (adjusted *p*-value: < 0.0001) compared to M4. Results from the MTT and LDH tests are in triplicate, and each line denotes the mean value. Magnification: x 50. DMEM: Dulbecco's Modified Eagle's Medium, M199: Medium 199, KHB: Krebs-Henseleit Buffer, FBS: fetal bovine serum, MTT: Thiazolyl Blue Tetrazolium Bromide, LDH: Lactic Dehydrogenase.

area, compared to the incubated medium results obtained for the metabolic profile of HEK293 cells, actually reflects the uptake rather than the secretion of glucose. This observation raises concerns regarding data interpretation if the aim of a given experiment was to target glucose in the secretome of HEK293 cells. It would subsequently be necessary to screen for similar effects in any other selected cell line.

Citric acid is an example of a compound that was introduced with FBS addition, as it was neither detected nor reported in the media formulations. However, given that the relative peak area of citric acid was below the secreted values for both cell types, it may not represent a hurdle for data interpretation. Finally, hypoxanthine was also introduced with FBS addition (M4), given that it was not detected in DMEM media alone. In this case, the addition of FBS may hinder the interpretation of the L6 cell secretome. As an example of our identification method, Fig. S2 shows how the presence of hypoxanthine was confirmed via AMRT, as well as through the identification of two fragment ions at a collision energy of 30 eV in the quality controls. Profiles for each metabolite across the five media combinations are shown in Fig. S3. Results for all the metabolites can be found in Supplementary Data.

3.6. *Influence of incubation on DMEM + GlutaMAX™*

As discussed before, when evaluating the secretome via metabolomics approaches, an understanding of the relative value of a given metabolite from the contributing growth media supplemented to the cells should be included. However, it is unclear whether this medium should be refrigerated or incubated. Multiple factors may affect the observed metabolite profile, including storage of the culture media, exposure to light and/or humidity, and metabolite degradation, few of which have been examined. A combined quantitative and qualitative metabolomics study by Zang et al. [13] investigated the content of a failed media lot that resulted in a low viable cell density. Degradation and oxidation products were observed in their tested media. Additionally, media in solution compared to a chemically defined media powder exposed to heat and light indicated that the powder was more resistant to oxidative degradation compared to the solution [13]. The depleted medium (M5), prepared from powder, in the present study did not

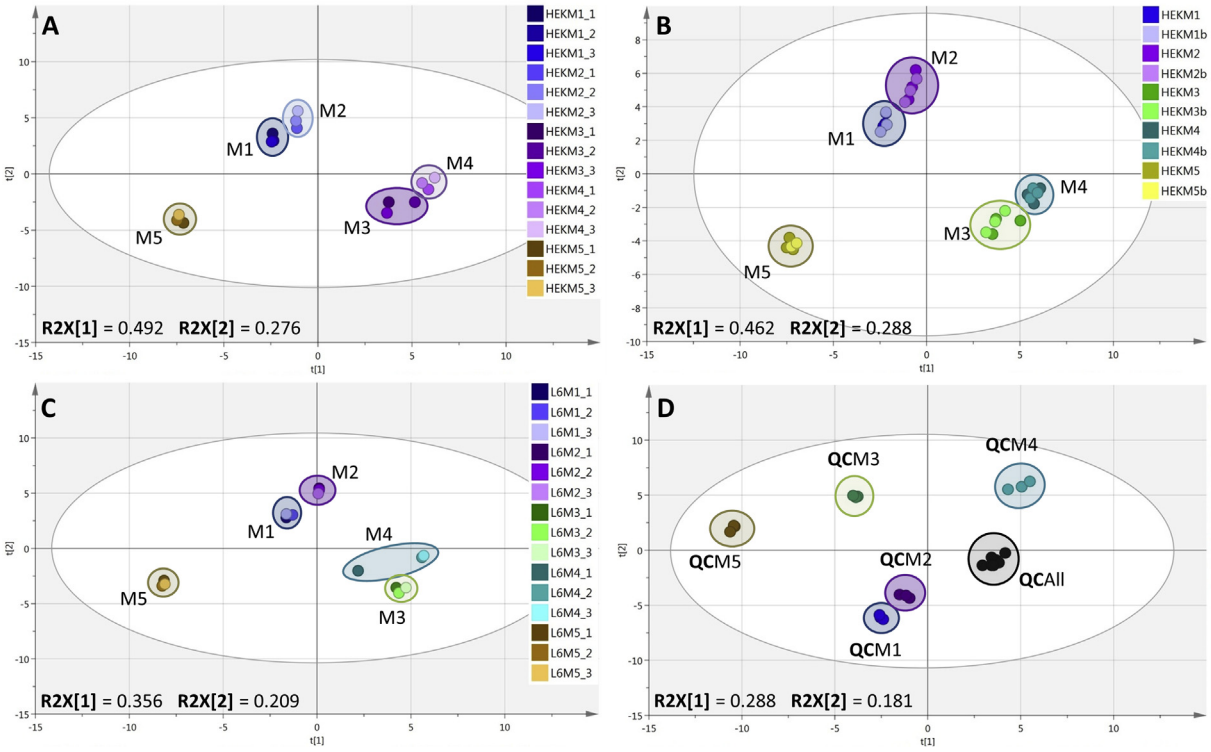

Fig. 5. Score plots of combined positive and negative ionization metabolomics datasets incorporating the 53 unique metabolites. **A.** Score plot of HEK293 cells for all five media types. **B.** Score plot of HEK293 cells run throughout the sequence based upon media type, compared to those run at the end of the sequence. These samples overlap; hence there was no instrumental drift. Samples run in triplicate overlap according to media type. **C.** Score plot of L6 cells for all five media. **D.** Score plot of QC samples representing each medium type alone along with the 3 QC-All samples run in triplicate. Circles around each cluster of samples is for visual purposes and do not represent any statistical value (*e.g.*, 95% confidence interval).

evidence the same variability across the replicates as the ones in solution; however, due to the low number of organic compounds any conclusive statement cannot be made.

Creek et al. [10] investigated the concentration changes of spent media (*i.e.*, a standard culture media for *T. brucei*, and their in-house Creek's minimal media) after 56 h of sub-culture (*i.e.*, cell growth) relative to fresh medium via their zicHILIC Orbitrap platform. Their optimized medium was able to reflect the intracellular changes in tryptophan and phenylalanine concentration much better compared to the commercial media for their respective analysis. Interestingly, the authors suggest decreasing HEPES to 10 mM in order to reduce LC interference; in the present study HEPES present in M5 was at a concentration of 5 mM and completely absent from M199 and DMEM.

Based on the PCA score plot profile of Fig. 2 (B), we selected M3 to further investigate the effects of incubation on the compounds present in one of the media. Plate weight did not change before and after incubation or refrigeration, showing no evaporation of the medium in both conditions. The PCA score plot showed no discernible cluster of samples (Fig. 7. A), which reflected no major changes due to incubation. Further analysis was performed to identify compounds marginally affected by incubation. The score plot (Fig. 7. B) obtained for the PLS-DA model (1 latent variable, $R^2(Y) = 0.84$, $Q^2 = 0.76$) between both classes was able to distinguish incubated and non-incubated samples. Two metabolites, pyroglutamate and glutamine, were identified as major contributors to the separation between classes according to the VIP (Fig. 2. C). Differences between these modes could be a result of the non-enzymatic breakdown of glutamine, to form pyroglutamate and ammonia as by-products [21], which could have been accelerated by placing the samples in incubated conditions-especially in liquid form. However, it has also been shown that pyroglutamate can be formed spontaneously from glutamate [22]. The production of ammonia from the aforementioned reaction, although not screened for in the present study, can have negative consequences in culture conditions relating to the cells' secretion ability, and result in inefficient cell growth [23]. According to its formulation, DMEM does not contain glutamine or glutamate; however, the dipeptide form of glutamine (alanyl-L-glutamine) marketed as GlutaMAX™ has been reported as a more stable form of glutamine in the current formulation [21,24]. In MacIntyre et al., passage 11 conditioned media of human foreskin fibroblasts showed higher concentrations of alanine, and lower levels of GlutaMAX™. The authors suggest that this observation is due to the hydrolyzed GlutaMAX™ dipeptide during the conditioning step to form its constituents - alanine and glutamine. Glutamine was unchanged however, possibly due to uptake by the human foreskin fibroblasts.

Altogether, incubation of M3 did not profoundly alter the targeted metabolites at levels that would compromise the interpretation of the results from the present study. However, the changes observed for glutamine and pyroglutamate, though small, suggest that incubation may need to be controlled whenever possible. Additionally, more unstable metabolites may appear when using non-targeted metabolomics approaches.

3.7. Targeted validation outcome

Targeted validation is often the next step for a metabolomics-based experiment [25,26]. Thus, we performed a targeted LC-MS/MS analysis with the aim of validating the observed secretory metabolic profiles of the L6, HEK293 cells as well as from the cell-free media of the metabolomics study. For the validation

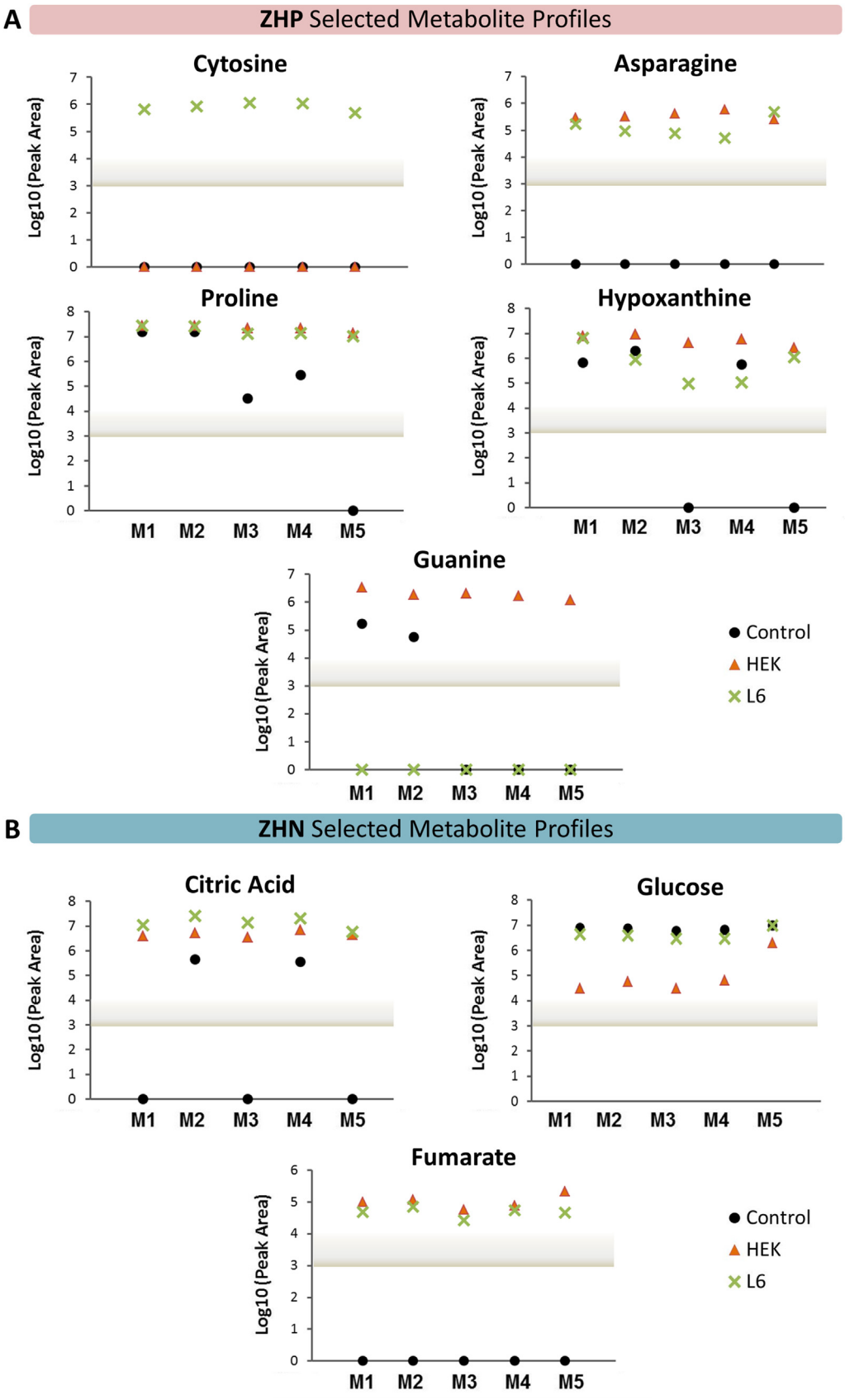

Fig. 6. Selected metabolite profile examples from positive (ZHP) and negative (ZHN) ionization acquisition modes. Values are presented as means of log transformed (base of 10) data. Control represents the incubated medium for each case. (n = 3). The shaded area is an estimated region for the limit of detection for the $\log_{10}$(Peak Area). Control: incubated cell-free media.

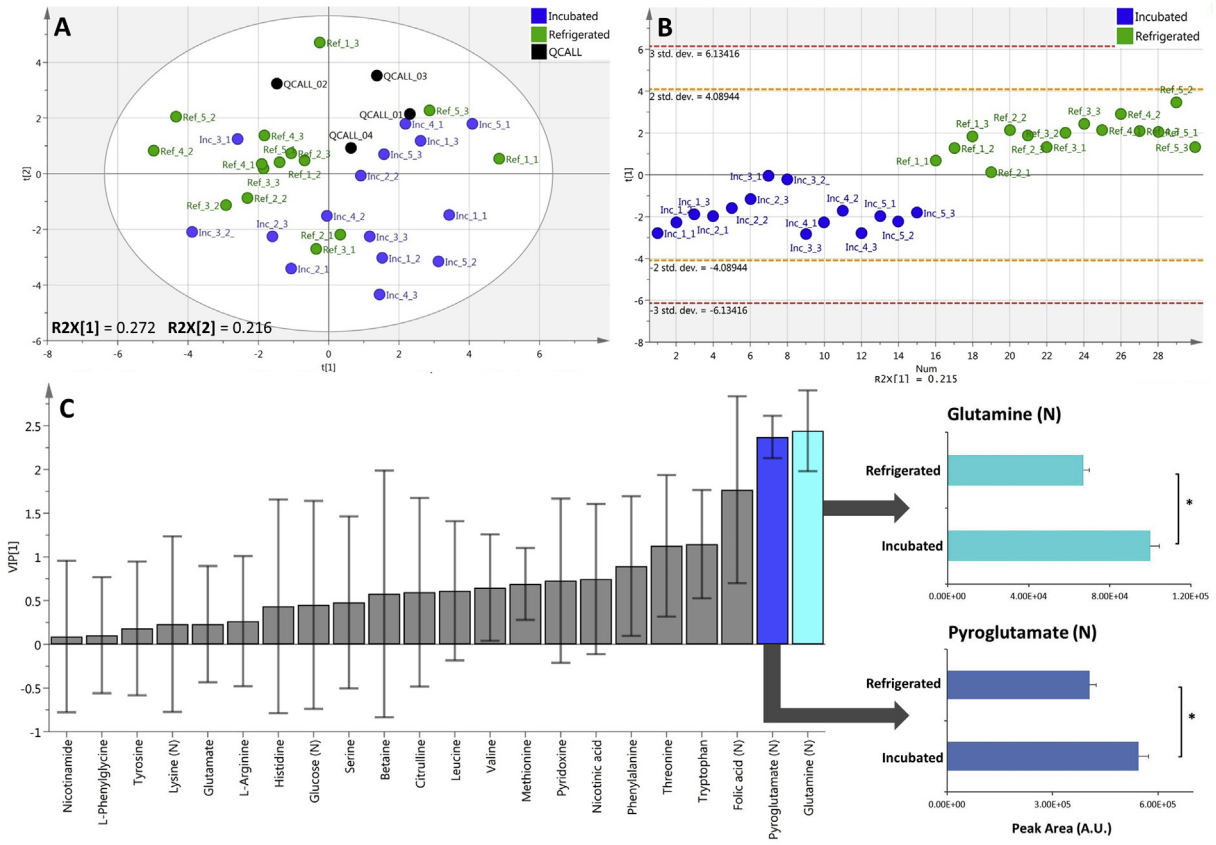

Fig. 7. Overview of detected metabolites (N: 22; ZHP and ZHN) comparing 24 h incubation *vs.* refrigeration of medium 3 (DMEM + GlutaMAX™). **A.** PCA score plot of all samples including QC-All. Partial separation of the two main classes (incubated and refrigerated) is observed, however, there is general variability across the samples tested. **B.** PLS-DA (1 latent variable) of two experimental conditions shows distinct separation of classes (R2Y (cum): 0.841, Q2 (cum): 0.758). **C.** Variable Importance in Projection (VIP) plot generated from (B) shows pyroglutamate and glutamine (VIP score > 2.0) as potential metabolites that are most affected by incubation. Values in bar charts are shown as means + SD (n = 3). *p < 0.001. DMEM: Dulbecco's Modified Eagle's Medium, ZHP: zicHILIC positive ionization, ZHN: zicHILIC negative ionization, N : Negative mode ionization.

experiments, cells were grown independently from the metabolomics experiment. The LDH activity of the additional cell-culturing experiment is provided in Fig. S4. The L6 cells showed a similar profile to the initial experiment. Compared to the control (M4), M5 had the highest significant cell death (adjusted *p*-value: < 0.0001) followed by M3 (*p*-value = 0.0004), and M1 (*p*-value = 0.0008). As in the metabolomics experiment, no differences were found for HEK293 cells.

For the purposes of the current study, we selected three compounds and their associated isotope labelled internal standards (arginine, folic acid, methionine). We also included citrulline and ornithine, which together with arginine form part of the urea cycle. Based upon the previous experiments, we chose to continue with incubated media as our control, because this is more representative of the initial conditions to which the cells are exposed. Results for the measured metabolites are presented in the Supplementary Data file.

Scatter plots of log transformed data of the selected metabolites from both the metabolomics and targeted approaches are shown in Fig. 8. Citrulline (Fig. 8A), arginine (Fig. 8B), and ornithine (Fig. 8C) showed variations in their respective metabolic profiles from the metabolomics approach. In both experiments, arginine was detected in M199 and DMEM containing media (M1-M4), whose formulations had reported concentrations of 3.32×10^{-1} mM and 3.98×10^{-1}mM, respectively. The only discrepancy between both profiles was the lack of secretion of arginine by HEK293 cells in M5. This difference can be attributed to the aforementioned growth variability of these cells. In the case of citrulline, targeted validation showed the presence of this compound in all samples, even in the ones where it was not detected via metabolomics (M1, M3 and M5). This observation can be attributed to the decreased sensitivity of metabolomics relative to targeted approaches. A similar observation was made with ornithine, where detection in the M1 and M5 profiles was achieved via the targeted approach.

Folic acid (Fig. 8D) was in the M199 and DMEM formulations, based on the manufacturer's description, at a concentration of 2.27×10^{-5} and 9.07×10^{-3} mM, respectively. The lower concentration of folic acid in M199 resulted in the compound not being detected in the media (M1 and M2), either alone or in the cells. However, in M3 and M4 there was a general overlap between both cell lines and the media. The validation approach confirms both the presence and profile of this compound. Finally, methionine (Fig. 8E) was present in M199 and DMEM at concentrations of 1.01×10^{-1} and 2.01×10^{-1} mM, respectively. This was strongly reflected in both the metabolomics and targeted approaches with controls showing a higher relative abundance than the secretome of the cells (M1-M4). Interestingly, the targeted approach using the labelled internal standard showed a more distinct change of methionine from M1-2 to M3-4, reflective of this increased supplemented concentration of the formulation. This was matched in the secretory profile of the cells. Both methodological approaches did not detect methionine in the control of M5; while in both cases methionine was more largely secreted by L6 cells.

Overall, the metabolic panels from the targeted validation

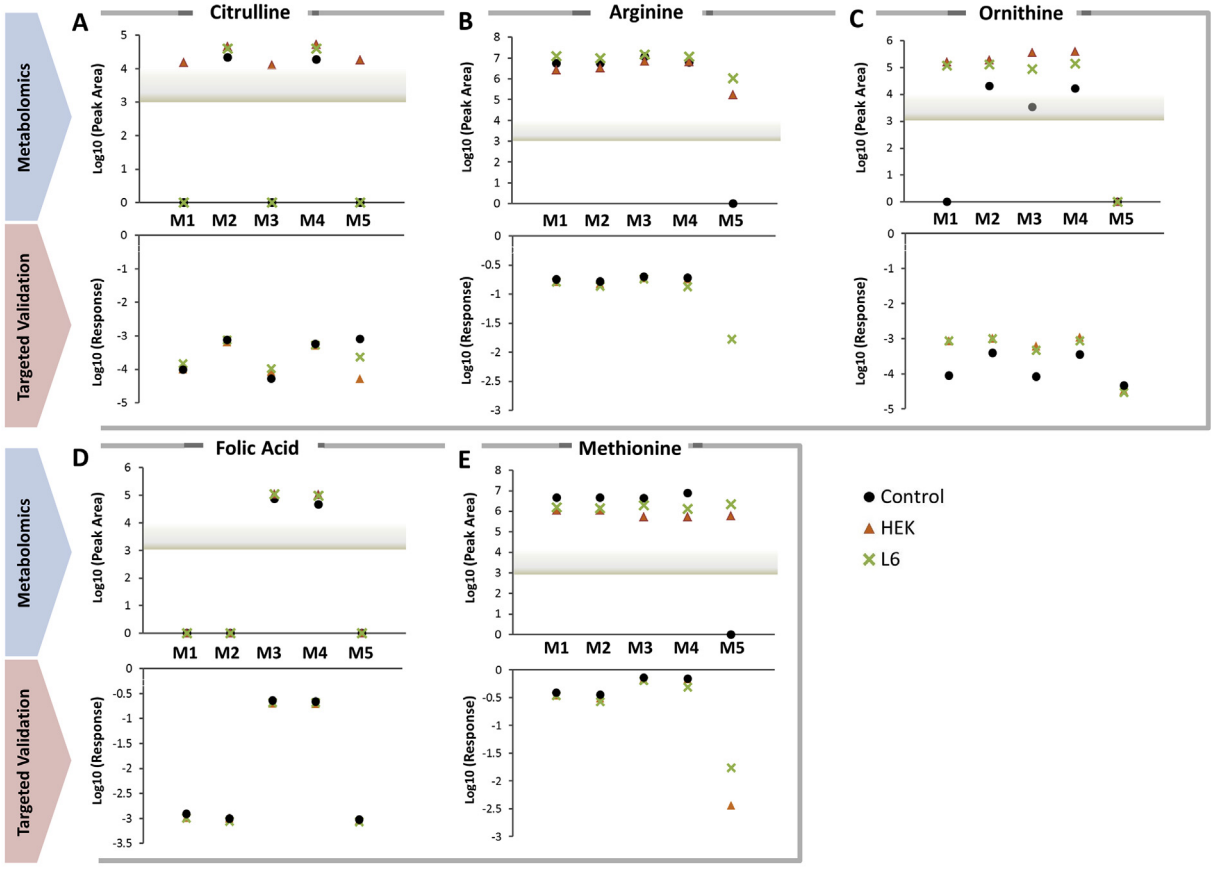

Fig. 8. Selected metabolite profiles from the metabolomics experiment compared with the corresponding profiles from the targeted validation (LC-MS/MS). Control: incubated cell-free media. An absent point from the validation scatter plot (log_{10} (response)) indicates that the compound was not detected in the three biological replicates. Values are presented as means of log transformed (base of 10) data. The shaded area represents an estimated region for the limit of detection for the log_{10}(Peak Area) in the metabolomics experiment.

corresponded with their respective metabolomics counterparts. Additionally, the validation results obtained from an independent experiment show the reliability of the metabolomics approach.

3.8. Additional avenues for consideration

There are a range of post-hoc normalization techniques that can be used to address some of the analytical challenges post-acquisition to adjust for observed sample-to-sample variance. These include, cell count, total protein content, DNA content, total ion current, wet weight, single metabolites from the secretome, or cell line, otherwise known as housekeeping metabolites [3,27,28]. In the targeted validation study, we measured protein content using a BCA assay kit and found that normalization did not affect the observed metabolic profiles (data not shown). Interestingly, fluorescence-activated cell sorting (FACS) can cause significant stress to the intracellular environment of the cells [29]. This effect is due to a combination of temperature and pressure alterations, in addition to the use of a nutrient depleted buffer. Accordingly, while FACS sorting is routinely performed for sorting cell populations, there can be unintentional effects reflected at the metabolite level that should be incorporated into the experimental design [29]. Another potential area of interest is the testing of spent medium (*i.e.*, medium that is usually discarded after sub-culture) as shown in Creek et al. [10], as well as the application of our experimental protocol to cell lysates (*i.e.*, intracellular content). As one potential avenue to address the effects of FBS supplementation in the media upon observed metabolite profiles, dialyzed FBS can be employed. It is likely that this would minimize the serum contribution of low molecular weight compounds to the cell secretome. However, the potential effects upon cell viability would have to be evaluated on a case-by-case basis.

4. Conclusion

There are a variety of protocols associated with each respective cell line; these can include, but are not limited to, incubation time, incubation temperature, quantity, batch and species origin of FBS, number of PBS washes, and harvesting procedures. Inevitably, some of these steps will be difficult to standardize. It is therefore important to ensure that the appropriate experimental controls are used in order to maximize biologically interpretable and reproducible findings. We have demonstrated that the media itself, even after 2% FBS addition, is the primary driver of the clustering of the cell line samples. Nonetheless, it is necessary to account for FBS-associated contributions to the observed metabolite levels. By performing a targeted validation of selected metabolites, we were able to show the reliability of the metabolomics approach. Taken together, our findings show that different metabolite secretory patterns will arise from the different media combinations, which can ultimately affect the interpretability of the resulting data. These effects need to be evaluated on a metabolite-by-metabolite basis, highlighting the need to perform rigorous pilot studies to characterize the cell culturing system prior to the initiation of metabolomics experiments. Based upon the present work, we suggest the following experimental considerations:

1. Multiple media combinations (including a range of FBS percentage) should be considered when evaluating a particular cell line.
2. Media combinations (*i.e.*, cell-free) should be plated separately, and incubated/treated in the same experimental conditions as the cells. Non-incubated media combinations can also be used as controls; however, this may not be appropriate for the full panel of screened metabolites.
3. Ideally, a compromise between cell death and optimal detection of metabolites should be evaluated. This approach is necessary to avoid, as much as possible, batch-specific FBS contributions that can render experiments irreproducible. These effects will be dependent upon the metabolites of interest.

Finally, the analytical performance of each compound of interest, within the selected cell-culturing conditions, should be evaluated and optimized accordingly to ensure robust outcomes. The implementation of these considerations when designing a cell culture secretome metabolomics experiment should increase the precision of the results and ultimately the interpretability and reliability of the experiment.

Conflicts of interest

The authors declare no conflict of interest.

Acknowledgments

This work was supported by the Novo Nordisk Foundation (TrIC NNF15CC0018486 and MSAM NNF15CC0018346) and the ChAMP (Centre for Allergy Research Highlights Asthma Markers of Phenotype) consortium which is funded by the Swedish Foundation for Strategic Research, the Karolinska Institutet, AstraZeneca & Science for Life Laboratory Joint Research Collaboration, and the Vårdal Foundation. CEW was supported by the Swedish Heart Lung Foundation (HLF 20150640). NJP was supported by a Marie Skłodowska-Curie Fellowship [H2020-MSCA-IF-2015, 704978].

Appendix A. Supplementary data

Supplementary data related to this article can be found at https://doi.org/10.1016/j.aca.2018.04.034.

References

[1] F.G. Hopkins, An address on the dynamic side of biochemistry: delivered to the physiological section of the british association for the advancement of science, Br. Med. J. 2 (1913) 713–717.
[2] E.W. Taylor, 1999 E.B. Wilson lecture: the cell as molecular machine, Mol. Biol. Cell 12 (2001) 251–254.
[3] L.P. Silva, P.L. Lorenzi, P. Purwaha, V. Yong, D.H. Hawke, J.N. Weinstein, Measurement of DNA concentration as a normalization strategy for metabolomic data from adherent cell lines, Anal. Chem. 85 (2013) 9536–9542, https://doi.org/10.1021/ac401559v.
[4] P. Hunter, Reading the metabolic fine print. The application of metabolomics to diagnostics, drug research and nutrition might be integral to improved health and personalized medicine, EMBO Rep. 10 (2009) 20–23, https://doi.org/10.1038/embor.2008.236.
[5] J.K. Nicholson, J.C. Lindon, Systems biology: metabonomics, Nature 455 (2008) 1054–1056, https://doi.org/10.1038/4551054a.
[6] K. Duval, H. Grover, L.-H. Han, Y. Mou, A.F. Pegoraro, J. Fredberg, Z. Chen, Modeling physiological events in 2D vs. 3D cell culture, Physiology 32 (2017) 266–277, https://doi.org/10.1152/physiol.00036.2016.
[7] P. Mukherjee, S. Mani, Methodologies to decipher the cell secretome, Biochim. Biophys. Acta 1834 (2013) 2226–2232, https://doi.org/10.1016/j.bbapap.2013.01.022.
[8] A. Halama, Metabolomics in cell culture—a strategy to study crucial metabolic pathways in cancer development and the response to treatment, Arch. Biochem. Biophys. 564 (2014) 100–109, https://doi.org/10.1016/j.abb.2014.09.002.
[9] T.J. Causon, S. Hann, Analytica Chimica Acta Review of sample preparation strategies for MS-based metabolomic studies in industrial biotechnology, Anal. Chim. Acta 938 (2016) 18–32, https://doi.org/10.1016/j.aca.2016.07.033.
[10] D.J. Creek, B. Nijagal, D.-H. Kim, F. Rojas, K.R. Matthews, M.P. Barrett, Metabolomics guides rational development of a simplified cell culture medium for drug screening against Trypanosoma brucei, Antimicrob. Agents Chemother. 57 (2013) 2768–2779, https://doi.org/10.1128/AAC.00044-13.
[11] S. Nonnis, E. Maffioli, L. Zanotti, F. Santagata, A. Negri, A. Viola, S. Elliman, G. Tedeschi, Effect of fetal bovine serum in culture media on MS analysis of mesenchymal stromal cells secretome, EuPA Open Proteomics 10 (2016) 28–30, https://doi.org/10.1016/j.euprot.2016.01.005.
[12] D.A. MacIntyre, D. Melguizo Sanchís, B. Jiménez, R. Moreno, M. Stojkovic, A. Pineda-Lucena, Characterisation of human embryonic stem cells conditioning media by 1H-nuclear magnetic resonance spectroscopy, PLoS One 6 (2011), https://doi.org/10.1371/journal.pone.0016732 e16732.
[13] L. Zang, R. Frenkel, J. Simeone, M. Lanan, M. Byers, Y. Lyubarskaya, Metabolomics profiling of cell culture media leading to the identification of riboflavin photosensitized degradation of tryptophan causing slow growth in cell culture, Anal. Chem. 83 (2011) 5422–5430, https://doi.org/10.1021/ac2009492.
[14] M. Čuperlović-Culf, D.A. Barnett, A.S. Culf, I. Chute, Cell culture metabolomics: applications and future directions, Drug Discov. Today 15 (2010) 610–621, https://doi.org/10.1016/j.drudis.2010.06.012.
[15] S. Naz, H. Gallart-Ayala, S.N. Reinke, C. Mathon, R. Blankley, R. Chaleckis, C.E. Wheelock, Development of a liquid chromatography–high resolution mass spectrometry metabolomics method with high specificity for metabolite identification using all ion fragmentation acquisition, Anal. Chem. 89 (2017) 7933–7942, https://doi.org/10.1021/acs.analchem.7b00925.
[16] A.A. Stepanenko, V.V. Dmitrenko, HEK293 in cell biology and cancer research: phenotype, karyotype, tumorigenicity, and stress-induced genome-phenotype evolution, Gene 569 (2015) 182–190, https://doi.org/10.1016/j.gene.2015.05.065.
[17] A. Yap, S. Nishiumi, K.-I. Yoshida, H. Ashida, Rat L6 myotubes as an in vitro model system to study GLUT4-dependent glucose uptake stimulated by inositol derivatives, Cytotechnology 55 (2007) 103–108, https://doi.org/10.1007/s10616-007-9107-y.
[18] X. Zheng, H. Baker, W.S. Hancock, F. Fawaz, M. McCaman, E. Pungor, Proteomic analysis for the assessment of different lots of fetal bovine serum as a raw material for cell culture. Part IV. Application of proteomics to the manufacture of biological drugs, Biotechnol. Prog. 22 (2008) 1294–1300, https://doi.org/10.1021/bp060121o.
[19] C. Rauch, E. Feifel, E.-M. Amann, H.P. Spötl, H. Schennach, W. Pfaller, G. Gstraunthaler, Alternatives to the use of fetal bovine serum: human platelet lysates as a serum substitute in cell culture media, ALTEX 28 (2011) 305–316.
[20] X. Zheng, H. Baker, W.S. Hancock, F. Fawaz, M. McCaman, E. Pungor, Proteomic analysis for the assessment of different lots of fetal bovine serum as a raw material for cell culture. Part IV. Application of proteomics to the manufacture of biological drugs, Biotechnol. Prog. 22 (2008) 1294–1300, https://doi.org/10.1021/bp060121o.
[21] J.R. Masters, G.N. Stacey, Changing medium and passaging cell lines, Nat. Protoc. 2 (2007) 2276–2284, https://doi.org/10.1038/nprot.2007.319.
[22] C.B. Park, S.B. Lee, D.D.Y. Ryu, L-pyroglutamate spontaneously formed from l-glutamate inhibits growth of the hyperthermophilic archaeon sulfolobus solfataricus, Appl. Environ. Microbiol. 67 (2001) 3650–3654, https://doi.org/10.1128/AEM.67.8.3650-3654.2001.
[23] M. Jagušić, D. Forčić, M. Brgles, L. Kutle, M. Šantak, M. Jergović, L. Kotarski, K. Bendelja, B. Halassy, Stability of minimum essential medium functionality despite l-glutamine decomposition, Cytotechnology 68 (2016) 1171–1183, https://doi.org/10.1007/s10616-015-9875-8.
[24] Thermo Fisher scientific Inc, GlutaMAX media, Thermo Fish. Sci. (2015). https://tools.thermofisher.com/content/sfs/brochures/glutamax-product-brochure.pdf. (Accessed 27 October 2017).
[25] A. Checa, J. Saurina, Metabolomics and PDO, in: Compr. Anal. Chem, Elsevier, 2013, pp. 123–143, https://doi.org/10.1016/B978-0-444-59562-1.00006-2.
[26] J. Zhou, Y. Yin, Strategies for large-scale targeted metabolomics quantification by liquid chromatography-mass spectrometry, Analyst (Cambridge, U.K.) 141 (2016) 6362–6373, https://doi.org/10.1039/C6AN01753C.
[27] B. Cao, J. Aa, G. Wang, X. Wu, L. Liu, M. Li, J. Shi, X. Wang, C. Zhao, T. Zheng, S. Guo, J. Duan, GC–TOFMS analysis of metabolites in adherent MDCK cells and a novel strategy for identifying intracellular metabolic markers for use as cell amount indicators in data normalization, Anal. Bioanal. Chem. 400 (2011) 2983–2993, https://doi.org/10.1007/s00216-011-4981-8.
[28] C. Muschet, G. Möller, C. Prehn, M.H. de Angelis, J. Adamski, J. Tokarz, Removing the bottlenecks of cell culture metabolomics: fast normalization procedure, correlation of metabolites to cell number, and impact of the cell harvesting method, Metabolomics 12 (2016) 151, https://doi.org/10.1007/s11306-016-1104-8.
[29] I. Roci, H. Gallart-Ayala, A. Schmidt, J. Watrous, M. Jain, C.E. Wheelock, R. Nilsson, Metabolite profiling and stable isotope tracing in sorted subpopulations of mammalian cells, Anal. Chem. 88 (2016) 2707–2713, https://doi.org/10.1021/acs.analchem.5b04071.